IN-90-CR

P.41

PROGRESS REPORT

NAG 5 1282

DUST NEAR LUMINOUS ULTRAVIOLET STARS

prepared by

Richard C. Henry

Principal Investigator

March 1992

This progress report is provided as required by Grant NAG 5 1282 titled *IRAS-ADP Study of Dust Near Luminous Ultraviolet Stars* with Principal Investigator, R. C. Henry.

The bulk of the work under this grant has now been completed. The major results are all contained in a paper , "The Low Filling Factor of Dust in the Galaxy" (attached), by Jayant Murthy, H. J. Walker, and R. C. Henry. This paper has been submitted to the Astrophysical Journal.

It remains to study the individual clouds. We will carry out this work over the next year. Another major publication should result.

THE LOW FILLING FACTOR OF DUST IN THE GALAXY

JAYANT MURTHY[1], H. J. WALKER[2,3], AND R. C. HENRY[1]

[1]Department of Physics and Astronomy, The Johns Hopkins University, Baltimore, MD 21218

[2]SETI Institute, 2035 Landings Drive, Mountain View, CA 94043

[3]Rutherford Appleton Laboratory, Chilton, Didcot, Oxon, United Kingdom

Received Submitted Feb. 28

ABSTRACT

We have examined the neighborhood of 745 luminous stars in the *IRAS* Skyflux plates for the presence of dust heated by the nearby star. This dust may be distinguished from the ubiquitous cool cirrus by its higher temperature and thus enhanced 60 μm emission. We have found 123 dust clouds around only 106 of the stars with a volume filling factor of 0.006 and an intercloud separation of 46 pc. Nowhere do we find a region where the dust is smoothly distributed through the volume of space heated by the star and hence we place an upper limit of 0.05 cm^{-3} on the equivalent gas density in the intercloud regions.

The clouds, themselves, have an average density of 0.22 cm^{-3} (assuming a standard gas-to-dust ratio) and a radius of 1.9 pc, albeit with wide variations in their properties. We have tentatively identified these clouds with the warm, ionized medium of McKee and Ostriker. We have found two different scale heights of 140 and 540 pc for the number of clouds around different groups of stars which we have interpreted as evidence for different distributions of dust in and out of the galactic disk. The dust at higher altitudes also appears to be more uniformly distributed with galactic latitude.

Subject headings: interstellar: matter — nebulae: reflection

1. INTRODUCTION

One of the major achievements of the *Infrared Astronomical Satellite* (*IRAS*) was its survey of 96% of the sky in four wavelength bands centered at 12, 25, 60, and 100 μm (for details see the *IRAS* Explanatory Supplement [1985]). By far the most dominant component seen at 100 μm is emission from the cirrus (Low *et al.* 1984), dust that is heated by the interstellar radiation field (ISRF), and detailed surveys of the dust in our Galaxy, similar to the HI surveys (*eg,* Heiles 1975), can be made (see, for example, Boulanger and Perault 1988).

In this work, we have used the *IRAS* Skyflux plates to study the environment in the vicinity of 745 luminous stars. Dust near these stars will be heated by the stellar radiation field to higher temperatures than the cool cirrus, from which it may be distinguished by an enhanced 60/100 μm flux density ratio. Conversely, if there is no emission near these stars, or only emission from the cool cirrus along the line of sight, we may place limits on the amount of dust and, by extension, on the amount of matter near those stars. As the distances to the stars in our program are known (or can be estimated), the dust distribution around those stars provides a probe of the three-dimensional structure of the interstellar medium (ISM) in our Galaxy.

We have found dust clouds around 106 of the 745 stars in our survey for a number fraction of 0.14, slightly less than the value of 0.2 found by Van Buren (1989) for a smaller sample of stars near the Galactic plane. However, many of these clouds occupy only a small fraction of the total volume around each star, implying a much lower volume filling factor. We will reserve discussion of the individual clouds for a future paper, here discussing only the environment of the stars and its implications for the global morphology of the dust.

2. DATA ANALYSIS

As mentioned above, we have examined the *IRAS* Skyflux plates, which are binned in 2′ pixels with an effective resolution of 6′ at all four wavelengths, in the neighborhood of 745 stars, selected primarily from the *Bright Star Catalog* (Hoffleit 1982). Several regions (Table 1) were excluded from our analysis, including regions within 10° of the Galactic plane, where background subtractions become problematic, and several regions of known molecular cloud concentrations, such as Orion or Taurus. (These regions are identical to those excluded by Boulanger and Perault 1988.) The distribution of our target stars in galactic coordinates is shown in Figure 1. The spectral type, apparent magnitude, and observed B-V for each star were obtained from the *Bright Star Catalog*; the absolute magnitude, temperature, and intrinsic B-V were read from tables in Zombeck (1982); and the E(B-V), spectroscopic distance, and luminosity of the star were calculated from the other quantities.

Although virtually all of the emission in the *IRAS* Skyflux plates is due to dust (interplanetary, circumstellar, or interstellar), we are interested in only that part which is actually due to dust heated by the star in question. The remainder, consisting primarily of zodiacal light and the cool cirrus, must therefore be identified and subtracted. We attempted to develop an automated computer procedure to do this but found that, in practice, we were limited to removing only the smooth component of the background, leaving behind any discrete structures, whether associated with the star or not. The first step in our procedure was to select a region of typically 6.7° x 6.7° (201 x 201 pixels) centered on the star (this region was smaller if the star was near the edge of a plate) and divide it into blocks of 20 x 20 pixels. We then fit a grid consisting of the minimum values in each of the blocks by a quadratic surface, which formed our estimate of the smooth background contribution to the plate. In order to ensure that the background was not affected by large bright clouds completely filling a block, we rejected any pixels with intensities more than 3σ over the mean (of all the pixels) and repeated the procedure. An example of our fit is shown in Figure 2. We obtained an estimate of the quality of our fits from the rms deviations in a relatively flux-free region of each plate. These deviations are 0.14, 0.20, 0.15, and 0.31 MJy sr^{-1} in the 12, 25, 60, and 100 μm bands, respectively, and are on the same order as errors cited by other groups using similar procedures (*eg.* Boulanger *et al.* 1990).

The remaining emission in the plate consists of not only dust clouds heated by the star but also cool cirrus clouds only coincidentally in the same direction as the star, and we must differentiate between the two. Our selection criteria were that the cloud exist as a distinct entity in the 60 μm map (not necessarily centered on the star) and that the 60/100 μm ratio within the cloud increase toward the star. We have found 123 such clouds (Table 2) around 106 stars, ranging in size and brightness from the large, bright (and well-known) clouds around ζ Oph (HD 149757; Van Buren and McCray 1988) and α Cam (HD 30614; de Vries 1985) to those barely distinguishable from the background. In order to estimate the errors in this procedure, we have performed our search twice, with different people, and finding agreement in 649 out of the 745 total cases, or in 87% of the cases. This difference is, however, proportionately greater in the number of clouds as 123 clouds were found the first time and 169 the second, with agreement in 81 cases. Not only is there ambiguity in deciding whether a faint patch is due to emission from dust heated by the star but there are a significant number of bright features for which it was a subjective decision whether there was an increase in the 60/100 μm ratio toward the star or not. Nevertheless, despite these problems, it is clear that most of the stars in our survey do not have detectable dust clouds nearby.

Selection effects are important in our data and two of them are illustrated in Figure 3 where we have plotted the radius of the clouds as a function of distance from the Sun. The first of these biases is introduced through the finite spatial resolution of the instrument: distant clouds must be larger in order to be above the resolution limit (solid line in Figure 3). In addition to small clouds not being detected at large distances, the converse effect is also present. This is primarily due to our selection by apparent magnitude: the nearer stars tend to be less intrinsically luminous and thus will not illuminate a large cloud in its entirety. That this is a factor in our results is shown in Figure 4 where we have expressed the radius of the cloud as a fraction of the distance at which the stellar radiation field drops to the level of the ISRF. It should be noticed that the nearby clouds are not significantly smaller, in relation to the stellar luminosity, than those at greater distances. Another consequence of our selection by magnitude is that we automatically discriminate against stars in high obscuration regions where there are more likely to be dust clouds. Finally, as the more luminous stars will both dominate over the ISRF for a larger volume of space and will heat dust within that volume to higher temperatures, we will be more likely to detect clouds around those stars (Table 3). As a corollary, we will be more likely to observe dust clouds around more distant stars, which tend to be intrinsically brighter, but the clouds will be larger, due to the instrumental resolution.

In order to model the emission from the dust near the star, or to place upper limits on the amount present, we have simply set equal the heat input from the star into the dust, calculated using a Kurucz model (Kurucz 1979) of the appropriate temperature multiplied by a dust absorption profile from Draine and Lee (1984), and the radiation emitted by the dust as a function of the dust temperature, again using optical constants from Draine and Lee. The predicted signal in each of the *IRAS* bands was found by convolving the calculated dust emission profile with the instrument response function. In Figure 5, we have plotted the expected emission at 100 μm from stars of several spectral types placed in a uniformly distributed medium of density 0.1 cm^{-3} as a function of distance from the star. (The density of the dust is quoted here, and elsewhere in this work, in terms of the equivalent amount of HI, assuming the canonical gas to dust ratio of 5.8×10^{21} atoms cm^{-3} mag^{-1}[Bohlin, Savage, and Drake 1978]. Note that this is implicit in the Draine and Lee model.)

3. RESULTS AND DISCUSSION

3.1. Cloud Properties

In the present work, we are concerned only with the group properties of the clouds listed in Table 2 and so have used several approximations to characterize them. We have assumed spherical clouds with a radius given by the average length over two orthogonal axes (defined by the plate in question) at a distance from the exciting star such that the predicted 60/100 μm ratio is equal to the observed value (defined as the average over the entire cloud). The amount of dust in each cloud was estimated by calculating an emissivity per grain based on the ratio of the 60/100 μm emission in each pixel, dividing into the observed emission in that pixel, and summing over all the pixels in the cloud. Finally, the average density in the cloud was obtained by dividing by the volume.

We have tabulated the average properties of the detected clouds in Table 4. We find an average cloud radius of 1.9 pc and an average [equivalent HI] density of 0.2 cm^{-3}. However, there is a wide variation in cloud sizes and most have a radius of less than 0.5 pc and a density of less than 0.05 cm^{-3}, as may be seen from the histograms in Figures 6 and 7. The column density through one of these clouds is typically less than about 10^{19} cm^{-2}. Their properties are strongly reminiscent of the warm clouds (warm, ionized medium) in the McKee and Ostriker (1977) theory, of which one example may be the local cloud around our Sun (Bruhweiler and Vidal-Madjar 1987).

We can calculate an average intercloud distance by noting that the total volume of space probed in our program is 6.3×10^6 pc^3, where the volume probed by a star is defined to be that region in which the stellar radiation field exceeds the interstellar value. As we detect 123 clouds in this volume, this implies that there is one cloud per 5.1×10^4 pc^3 or that there is an average of 46 pc between clouds. This is much larger than the intercloud distance of 12 pc (for the warm, ionized clouds) in McKee and Ostriker (1977). The total volume of space occupied by our clouds is 4×10^4 pc^3 leading to a filling factor of 0.006, much lower than the 0.23 in the McKee-Ostriker theory.

This is a very low filling factor and it is important that we understand both what we are measuring and the uncertainties in our procedure. Unfortunately, because of our observational biases, we do not sample a complete cloud distribution at any point and it is difficult for us to estimate by how much we undercount the number of clouds. The average distance between clouds is only dependent on the inverse cube root of the number of clouds and is thus relatively robust; however the filling factor is dependent on the total volume of the clouds and thus may be in error by a considerable amount, although it is difficult to imagine that we are missing over 95% of the warm material. Our data are not consistent with the conclusion of Kulkarni and Heiles (1987), based on a number of $H\alpha$ measurements (see Reynolds 1990), that the filling factor of the warm gas was 0.5 and the filling factor of the warm ionized medium (WIM) was 0.11, unless the special environment we are probing has been cleared of dust by the stars themselves.

Considering our selection effects, it is difficult to know just which parameter is a true estimator of the cloud distribution and, pending further modelling, we have chosen to use the fraction of stars in our survey which heat nearby dust as our estimator. In the interest of less involved sentences, we will hereafter refer to this quantity as simply the fraction of stars with dust.

The latitude dependence of the fraction of stars heating dust is tabulated in Table 5 and illustrated in Figure 8, plotted as plus signs. This dependence is fit reasonably well by a cosecant law (solid line) except at the highest latitudes, where the sample size is small. If, however, we break the stars into groups, based on intrinsic luminosity, we find that only the less luminous stars (asterisks in Figure 8) follow a cosecant law. Not only do a greater fraction of the bright stars heat nearby clouds (plus signs in Figure 8), but the distribution falls off much more slowly with increasing galactic latitude, perhaps reflecting a more uniform distribution of dust once out of the plane of the Galaxy. It should be cautioned that a much more rigorous approach, including Monte Carlo simulations of the cloud distributions, will be necessary to ensure that our results are not simply due to selection effects.

The z dependence of the clouds is listed in Table 6 and plotted in Figure 9. The luminosity effects completely mask the relation with height above the galactic plane for the entire sample, as the fraction of intrinsically bright stars increases with distance, and we have only plotted the fraction of stars with dust for the two luminosity subdivisions in the Figure. Aside from the normalization, we find exponential scale heights of 540 pc for the fraction of luminous stars with dust and 140 pc for the less luminous stars, consistent with the idea of two different distributions being sampled by the different stars. These values are comparable to the scale heights of 100 – 500 pc found from surveys of HI (Lockman *et al.* 1986) and cold cirrus (Burton *et al.* 1986). There are, however, significantly more clouds far from the plane than would be expected from even a 500 pc scale height, perhaps due to radiation pressure from galactic plane stars (Franco *et al.* 1991).

3.2. Gas Densities

Probably one of the most important and secure results in this work is the low density around our program stars. We have calculated the density in a series of concentric circles around each of the 745 stars assuming that all the emission at 60 μm is due to thermal emission from dust uniformly distributed around the star, with optical constants from Draine and Lee (1984). An associated error for each point was calculated using the rms deviations of the background in the respective plate and a weighted average over all the stars was derived (Figure 10). (It is important to realize that what we call the density is, strictly, not the actual density but is instead an upper limit, including the effects of cool cirrus spatially distant from the star.) The density we derive around each star depends on both the amount of emission nearby and on the strength of the stellar radiation field while the σs of the density depend on the rms errors of the appropriate plate (essentially the same for all the plates), and on the stellar luminosity. Thus the errors will be least near the brightest stars and the average density will be dominated by the densities near those stars. Most of the contribution to this average comes from two stars (ζ Oph and Spica) for which there is enough emission at 60 μm combined with a strong enough stellar radiation field that they dominate the density and, if we exclude these two stars, the upper limit on the density drops from about 0.12 cm^{-3} to 0.05 cm^{-3} (dashed line).

Another view of this information is presented in Figure 11 where we have plotted the fraction of stars with a density lower than the abscissa in a volume of radius given by the ordinate; for example, the density of the matter within 6 pc of the central star is less than

0.1 cm^{-3} for 80% of the stars. The shape of the contours in the Figure are an artifact of our processing — as the distance from the star increases, we only use those stars for which the stellar radiation field is greater than the ISRF. Thus, at large distances from the central star, we are probing only intrinsically bright stars which will, as discussed above, have more restrictive limits on the amount of nearby dust. If we were to consider only those bright stars, the contours in Figure 11 would be even more restrictive near the star, emphasizing the paucity of dust in our survey.

The exact value of the density is dependent on several of our assumptions. The albedos in our model are near 0.5, as given by Draine and Lee (1984). There is, however, evidence that the grains are actually much blacker in the far-ultraviolet (Murthy, Henry, and Holberg 1991, Hurwitz, Martin, and Bowyer 1991) which would drive the densities to even lower values. It has become clear from many studies (see Desert *et al.* 1990 for a summary and references) that a significant part of the 60 μm emission arises from transient heating of small grains, which comprise only a small part of the entire dust population by mass. The Draine and Lee (1984) model does not include this emission and thus the actual density should again be lower. We have also assumed that there is no contribution to the heating from photons below 912 Å, perhaps not true for the low densities found in this work. On the other hand, we have ignored extinction by whatever material is between the star and the point under consideration which would lower the radiation field and thus the heating at that point, increasing the derived density. Finally, the derived gas density depends on the assumed value of the gas-to-dust ratio. We have used a constant ratio of 5.8×10^{21} atoms cm^{-3} mag^{-1} (Bohlin, Savage, and Drake 1978); however, there are strong indications that this value, in fact, varies by at least a factor of four in different directions (Burstein and Heiles 1978) and may vary even more near the luminous stars in our study.

A related issue is the amount of stellar energy which escapes the immediate vicinity of the star and contributes to the ionization and energetics of the gas in our Galaxy. The total amount of energy emitted in the *IRAS* bands by all of the dust clouds is 3.7×10^{36} ergs s^{-1} which is 10^{-4} of the total stellar emission. Assuming that about 50% of the total output from the dust is emitted in the *IRAS* bands (Desert *et al.* 1990), less than 1% of the stellar luminosity is reprocessed near the star, in accord with many other studies of the redistribution of stellar photons. These results are not affected even if we use all of the emission near the star (Figure 12), rather than just that part in the clouds identified.

Similar conclusions have been drawn by both Leisawitz and Hauser (1988), who have found, from a study of several OB clusters, that less than 10% of the stellar flux is absorbed within 50 pc of the stars, after the stars have moved away from their pre-natal molecular clouds, and by Reynolds (1990) from the high ionization in the local ISM (within 100 pc of the Sun). There are not enough nearby sources to maintain this ionization and therefore UV radiation from O and B stars in the galactic plane must be reaching the Solar neighborhood, implying that there must be paths of low optical depth over that distance.

4. SUMMARY

We have detected 123 clouds (Table 2) around 106 of a sample of 745 stars for a number fraction of 0.17. These clouds are similar in properties (summarized in Table 4) to those clouds which make up the warm, ionized medium of McKee and Ostriker (1977) and may form a subsample of that group. If we ignore selection effects, important as they may be in this work, we obtain an average intercloud separation of 46 pc and a volume filling factor of 0.006, much lower than the 0.23 in the McKee-Ostriker theory. There is very little material around the stars except for the clouds and we place upper limits of about 0.05 cm^{-3} on the average gas density, which is weighted heavily by the emission near the brightest stars in our survey. We note that this implies that the density of any smooth component of the ISM must be less than this value and that most of the matter must be in the form of discrete clouds, either the diffuse clouds we sample or cold, dark clouds. As a corollary, most of the stellar ionizing flux escapes the neighborhood of the stars into the ISM as a whole.

The latitude dependence of the clouds is fit reasonably well by a cosecant distribution, except at high galactic latitudes. If one restricts the sample to only the most luminous stars, the fall-off with increasing latitude is much less, perhaps reflecting a more uniform distribution of dust once out of the galactic disk. If we divide our sample into two groups based on luminosity, we find exponential scale heights of 140 and 540 pc for the less luminous and more luminous stars, respectively, again perhaps reflecting differing distributions of dust. We have also found significant numbers of clouds at quite large distances from the galactic plane.

If our tentative identification of these clouds with the warm, ionized medium is correct, studying their distribution will yield important clues to the nature of the ISM.

TABLE 1

REGIONS EXCLUDED IN OUR SURVEY

Name	Galactic Longitude	Galactic Latitude
Carina	245 < l < 275	-20 < b < -10
Cepheus	98 < l < 141	10< b < 22
Chamaeleon	290 < l < 305	-20 < b < -10
Galactic Plane	0 < l < 360	-10 < b < 10
LMC	273 < l < 286	-38 < b < -30
Lupus	315 < l < 360	10 < b < 30
Ophiuchus	l < 50	10 < b < 20
Orion	190 < l < 220	-22.5 < b < -10
Perseus	150 < l < 170	-32.5 < b < -10

TABLE 2 — continued

	HD	Sp. Type	l	b	V	dist. (pc)	r_c (pc)	d_c (pc)	dens (cm^{-3})	F_{12}	F_{25}	F_{60}	F_{100}
										(x 10^{-5} ergs s^{-1})			
	(1)	(2)	(3)	(4)	(5)	(6)	(7)	(8)	(9)	(10)	(11)	(12)	(13)
59	83754	B5V	248.7	27.8	5.1	169	0.5	0.5	1.44	2.9	2.3	1.4	1.3
60	89353	B9Ib	266.8	22.9	5.3	806	1.4	1.2	0.18	92.7	8.7	1.3	0.8
61	91355	B9	278.6	11.1	5.7	108	0.2	0.2	28.9	5.7	0.5	2.6	4.1
62	91356	B4	278.6	11.1	6.1	215	0.3	0.9	26.0	5.5	0.8	2.7	4.3
63	105383	B9V	296.0	11.5	6.4	125	0.5	0.2	3.57	19.0	11.3	8.0	5.8
64	105521	B3IV	294.4	20.9	5.5	935	1.9	4.3	3.15	4.9	2.4	3.5	4.7
65	105521	B3IV	294.4	20.9	5.5	935	2.4	2.3	0.47	7.1	4.2	4.0	3.0
66	108257	B3V	299.0	11.2	4.8	580	4.8	2.5	0.87	4.0	2.5	6.1	6.5
67	116658	B1III	316.1	50.8	1.0	162	0.8	1.9	0.25	8.6	8.8	5.8	2.3
68	119361	B8III	313.2	19.8	6.0	447	1.2	0.9	1.78	6.4	4.5	1.6	2.2
69	119605	G0Ib	321.0	44.8	5.6	816	1.4	0.8	0.92	3.2	3.6	1.4	1.5
70	120307	B2IV	314.4	19.9	3.4	433	0.9	3.6	0.97	4.4	2.7	2.5	2.0
71	120307	B2IV	314.4	19.9	3.4	433	1.1	3.0	0.40	4.4	1.9	2.7	1.9
72	120640	B2V	313.5	14.7	5.8	892	2.9	4.7	1.50	7.1	4.3	3.4	4.7
73	121263	B2IV	314.1	14.2	2.5	291	1.1	5.3	2.97	11.8	6.8	4.3	5.0
74	124771	B4V	306.9	-18.0	5.1	155	0.8	0.4	3.75	3.1	4.3	9.5	7.2
75	128220	O7III	20.1	64.9	8.5	3158	8.2	7.1	0.06	5.6	3.8	1.7	1.3
76	135742	B8V	352.0	39.2	2.6	54	0.1	0.2	3.96	12.9	6.5	2.3	1.5
77	141527	G0I	45.1	51.0	5.8	3526	8.1	1.6	0.06	66.3	10.0	1.9	1.2
78	149630	B9V	66.9	42.7	4.2	43	0.0	0.2	5.93	6.3	2.7	0.9	0.5
79	149757	O9V	6.3	23.6	2.6	168	1.0	7.9	10.8	19.4	14.6	15.3	20.7
80	151525	B9	22.9	29.8	5.2	71	0.1	0.2	20.8	5.9	34.9	1.8	2.3
81	153261	B2IV	330.7	-10.3	6.1	1135	2.0	5.4	2.47	8.8	4.4	3.2	3.9
82	157246	B1I	334.6	-11.5	3.3	688	3.0	9.8	0.91	7.8	7.9	6.1	6.4
83	157246	B1I	334.6	-11.5	3.3	688	3.6	13.1	1.70	10.7	6.3	6.5	9.0
84	158148	B5V	42.7	27.3	5.5	205	0.4	0.7	7.25	21.7	14.8	1.1	1.5
85	159082	B9V	35.0	22.9	6.4	121	0.3	0.2	10.6	6.3	2.4	2.5	3.0
86	163506	F2Ib	51.4	23.2	5.5	1111	3.5	0.3	0.14	114.5	35.8	4.8	2.1
87	166014	B9V	55.2	21.6	3.8	37	0.0	0.2	10.4	3.3	3.5	1.3	1.0
88	167257	B9V	343.1	-15.7	6.1	110	0.2	0.2	4.92	7.5	5.9	2.0	1.8

TABLE 2 — continued

	HD	Sp. Type	l	b	V	dist. (pc)	r_c (pc)	d_c (pc)	dens (cm^{-3})	F_{12}	F_{25}	F_{60}	F_{100}
										(x 10^{-5} ergs s^{-1})			
	(1)	(2)	(3)	(4)	(5)	(6)	(7)	(8)	(9)	(10)	(11)	(12)	(13)
89	167756	B0Ia	351.5	-12.3	6.3	3301	10.5	15.4	0.27	9.5	7.7	5.8	5.9
90	172958	B8V	60.8	15.7	6.4	282	0.5	0.3	2.96	-1.3	-0.2	1.8	1.7
91	175360	B8	12.5	-11.3	5.9	220	0.8	0.2	0.95	34.8	18.8	5.0	3.4
92	175876	O6	15.3	-10.6	6.9	2741	9.6	5.3	0.08	75.5	43.4	10.2	5.3
93	176502	B3V	70.9	16.0	6.2	1138	3.0	3.3	1.14	2.3	1.1	2.2	3.0
94	177817	B8IV	20.0	-10.7	6.0	327	0.8	0.4	1.82	19.0	15.5	5.0	4.1
95	181615	B2V	21.8	-13.8	4.6	356	0.7	1.7	1.41	174.7	31.6	5.1	2.7
96	181858	B3IV	29.1	-10.6	6.7	1524	2.8	1.9	0.17	6.5	5.4	2.7	1.7
97	184915	B0II	31.8	-13.3	4.9	689	1.4	7.5	2.41	8.5	10.5	3.5	3.8
98	186042	B8	2.1	-25.9	6.2	234	0.5	0.5	8.11	1.5	0.0	2.4	3.5
99	189775	B5III	86.0	11.5	6.2	541	0.9	0.9	3.55	106.1	16.7	3.6	3.5
100	191639	B1V	34.0	-21.7	6.5	1204	2.9	2.6	0.20	7.1	8.6	2.7	1.9
101	191692	B9II	41.6	-18.1	3.2	46	0.2	0.4	48.3	12.8	11.7	3.9	6.7
102	193924	B2IV	340.9	-35.2	1.9	213	0.4	3.9	3.19	9.3	7.1	2.6	2.3
103	193964	B9V	96.5	14.4	5.7	92	0.2	0.2	5.10	3.7	0.5	1.7	1.4
104	196519	B9III	328.4	-35.6	5.2	109	0.2	0.2	4.67	3.0	3.2	2.0	1.9
105	196740	B5IV	67.0	-10.3	5.0	228	0.7	0.7	2.41	4.1	2.5	3.0	3.1
106	199140	B2IIIv	72.8	-10.5	6.6	1858	4.3	2.0	0.07	4.0	1.8	4.0	1.8
107	204867	G0Ib	48.0	-37.9	2.9	229	0.5	0.8	2.04	4.2	5.4	1.7	1.8
108	209409	B7IV	57.4	-42.7	4.7	178	0.5	0.5	1.77	6.0	6.1	2.7	2.3
109	209833	B9V	84.5	-21.3	5.6	89	0.2	0.2	16.3	2.9	1.8	2.0	2.8
110	212710	B9V	120.2	24.1	5.3	73	0.1	0.3	76.3	1.8	2.4	0.8	1.7
111	212883	B2V	93.6	-17.0	6.5	1172	3.1	1.0	0.05	4.1	7.5	3.5	1.3
112	214168	B2V	96.4	-16.1	5.7	863	4.1	3.2	0.44	5.0	2.5	4.4	4.2
113	214680	O9V	96.7	-17.0	4.9	769	2.7	6.2	0.49	8.9	4.0	4.0	3.6
114	214680	O9V	96.7	-17.0	4.9	769	1.7	6.3	1.09	5.1	4.6	3.8	3.5
115	214993	B2III	97.7	-16.2	5.2	1031	3.6	3.9	0.24	9.8	4.7	4.1	3.2
116	216200	B3IV	100.0	-15.5	5.9	917	1.9	4.7	2.46	2.5	2.0	1.7	2.5
117	217101	B2IV	100.1	-18.5	6.2	1399	4.5	3.9	0.44	8.2	3.7	5.3	4.7
118	217675	B6III	102.2	-16.1	3.6	148	1.0	0.6	1.83	7.2	3.4	9.0	6.4

TABLE 3

STELLAR LUMINOSITY EFFECTS

	$L_* < 10^{37}$ ergs s^{-1}	$L_* > 10^{37}$ ergs s^{-1}
number of stars	550	195
number of stars heating dust	52	54
number of clouds	55	68
fraction of stars heating dust	0.09	0.28
average no. of clouds per star	1.06	1.26
average cloud radius (pc)	0.59	2.99

TABLE 6

DISTRIBUTION OF CLOUDS WITH HEIGHT ABOVE PLANE

	Total No. of Stars	No of Stars with Dust	Fraction of Stars with Dust
$z < 100$ pc	384	46	0.120
100 pc $< z <$ 200 pc	163	23	0.141
200 pc $< z <$ 300 pc	86	15	0.174
300 pc $< z <$ 400 pc	47	8	0.170
400 pc $< z <$ 500 pc	18	5	0.278
500 pc $< z <$ 1000 pc	36	7	0.194
1000 pc $< z$	11	2	0.182
	Stars of $L_* < 10^{37}$ ergs s^{-1}		
$z < 100$ pc	370	39	0.105
100 pc $< z <$ 200 pc	129	10	0.078
200 pc $< z <$ 300 pc	32	1	0.031
300 pc $< z <$ 400 pc	10	0	0.000
400 pc $< z <$ 500 pc	2	1	0.500
500 pc $< z <$ 1000 pc	7	1	0.143
1000 pc $< z$	0	0	-
	Stars of $L_* > 10^{37}$ ergs s^{-1}		
$z < 100$ pc	14	7	0.500
100 pc $< z <$ 200 pc	34	13	0.382
200 pc $< z <$ 300 pc	54	14	0.259
300 pc $< z <$ 400 pc	37	8	0.216
400 pc $< z <$ 500 pc	16	4	0.250
500 pc $< z <$ 1000 pc	29	6	0.207
1000 pc $< z$	11	2	0.182

REFERENCES

Bohlin, R. C., Savage, B. D., and Drake, J. F. 1978, ApJ, 224, 132.

Boulanger, F., and Perault, M. 1988, ApJ, 330, 964.

Boulanger, F., Falgarone, E., Puget, J. L., and Helou, G. 1990, ApJ, 364, 136.

Bruhweiler, F. C., and Vidal-Madjar, A. 1987, in *Exploring the Universe with the* IUE *Satellite,* ed. Y. Kondo (Dordrecht: Reidel), p. 467.

Burstein, D., and Heiles, C. 1978, ApJ, 225, 40.

Burton, W. B., Walker, H. J., Deul, E. R., Jorgenleen, A. W. W. 1986, in *Light on Dark Matter,* ed. F. P. Israel (Dordrecht: Reidel), 357.

de Vries, C. P. 1985, A&A, 150, L15.

Desert, F. X., Boulanger, F., and Puget, J. L. 1990, A&A, 237, 214.

Draine, B. T., and Lee, H. M. 1984, ApJ, 285, 89.

Franco, J., Ferrini, F., Ferrara, A., and Barsella, B. 1991, ApJ. 366,443

Heiles, C. 1975, ApJS, 20, 37.

Hoffleit, D. 1982, *The Bright Star Catalog, 4^{th} Revised Edition,* Yale Univ. Obs. (New Haven)

Hurwitz, M., Bowyer, S., and Martin, C. 1991, ApJ 372, 167.

Kulkarni, S. R., and Heiles, C. 1987, in *Interstellar Processes,*ed. D. J. Hollenbach and H. A. Thronson, Jr. (Dordrecht: Reidel), p 87.

Kurucz, R. 1979, ApJS, 40, 1.

Leisawitz, D. and Hauser, M. G. 1988, ApJ 332, 954

Lockman, F. J., Hobbs, L. M., and Shull, J. M. 1986, ApJ, 301, 380.

Low, F. J., *et al.* 1984, ApJ 278, L19.

McKee, C. F., and Ostriker, J. P. 1977, ApJ, 218, 148.

Murthy, J., Henry, R. C., and Holberg, J. B. 1991, ApJ 383, 198.

Reynolds, R. J. 1990, ApJ 345, 811.

Reynolds, R. J. 1990, Proc. IAU 139, in *The Galactic and Extragalactic Background Radiation,* ed. S. Bowyer and C. Leinert, p 157.

Van Buren, D. 1989, ApJ, 338, 147.

Van Buren, D. and McCray, R. 1988, ApJ 329, L03.

Zombeck, M. V. 1982, *Handbook of Space Astronomy and Astrophysics*, Cambridge University Press (Cambridge)

FIGURE CAPTIONS

FIG. 1 — The distribution of the stars in our program in galactic coordinates is shown. Those stars around which we have found dust clouds are plotted as asterisks. Note that we have excluded several regions including the galactic plane, Orion and Taurus (see Table 1).

FIG. 2 — A cut through the original Skyflux plate is shown (upper line) with our fit to the background emission (smooth line). The lower line shows the residual emission. Some of the overall curvature in the original plate has been removed, without affecting the discrete features.

FIG. 3 — The radius of each of our clouds is plotted as a function of distance from the Sun. The lower envelope of these radii is due to the finite spatial resolution of the instrument, shown by the solid line. The nearby stars to the Sun are, in general, too intrinsically faint to illuminate large clouds in their entirety.

FIG. 4 — The radius of the cloud divided by the distance at which the stellar heating drops to the level of the ISRF (R_S) is plotted against distance from the Sun. From this plot, we see that the tendency for the nearby detected clouds to be smaller is probably due to the lower luminosities of the closer stars and thus is an observational artifact.

FIG. 5 — The emission seen from the dust at the given distance from the star is plotted for several different spectral types, assuming a uniform dust distribution of density 0.1 cm^{-3}. The radiation field from a hot star may light up dust clouds for many parsecs around.

FIG. 6 — A histogram of the number of clouds as a function of radius is plotted. The bin size is 0.1 pc and the last bin contains all clouds of radius 10 pc or greater. Despite the spatial resolution of the instrument, which places a stringent lower limit on the size of a cloud which can be detected (depending on distance), this distribution is heavily peaked to smaller clouds.

FIG. 7 — A histogram of the density of the clouds is plotted in 0.5 cm^{-3} bins. The distribution is heavily weighted to less dense clouds. The last bin contains all densities of 10 cm^{-3} or higher.

FIG. 8 — The fraction of stars heating nearby dust clouds is plotted as a function of latitude (plus signs). This distribution is fit reasonably well by a cosecant law (solid line). We have divided the stars into two groups based on whether their luminosity was less than or greater than 10^{37} ergs s^{-1} and plotted the latitude dependence of the clouds around each group of stars as asterisks and diamonds, respectively. Although the clouds around the less luminous stars (which lie largely in the galactic plane) still are consistent with a cosecant law, the clouds around the brighter stars appear to follow a much flatter distribution, albeit with poorer statistics, perhaps indicating a more uniform distribution of dust away from the plane.

FIG. 9 — The *z* dependence of the fraction of stars with clouds is plotted for stars with a luminosity less than 10^{37} ergs s^{-1} (asterisks) and for those with a greater luminosity (plus signs). The two groups follow different distributions and the best-fit (arbitrarily weighting each point by the square root of the number of stars in that bin) exponential distributions to each (solid lines) have scale-heights of 140 and 540 pc, respectively. This may reflect two populations of dust, one in the plane of the Galaxy (where the cooler stars in our survey tend to lie) and another with a more extended distribution. We detect several clouds at distances of more than 1kpc from the galactic plane, more than would be expected even with a scale height of 500 pc for the dust.

FIG. 10 — The upper limits on the density (using the 60 μm data) near each of the stars have been weighted by the appropriate error bars and summed to yield an average upper limit on the density as a function of distance from the star (solid line). This density is heavily weighted by two stars (ζ Oph and Spica), both of which have nearby dust clouds, and if we exclude them, we find a much lower average upper limit of 0.05 cm^{-3} (dashed line).

FIG. 11 — Another view of the low densities near the stars in our survey is to show the fraction of stars with densities below the given value. The change in the slope of the contours is caused by our only including stars for which the heat input into the dust exceeds the interstellar value and thus, as we probe further away from the star, only the most luminous stars — which have better upper limits — are included. At 5 pc from the star, we see that the upper limit on the gas density is less than 0.05 cm^{-3} for about 50% of the stars and less than 0.1 cm^{-3} for about 80% of the stars (including those stars with dust clouds detected nearby).

FIG. 12 — The emission within a series of circles around the central star is plotted as function of the radius of the circle as a percentage of the total stellar luminosity. Even within 10 pc of the star, much less than 1% of the stellar flux is emitted within the *IRAS* bands.

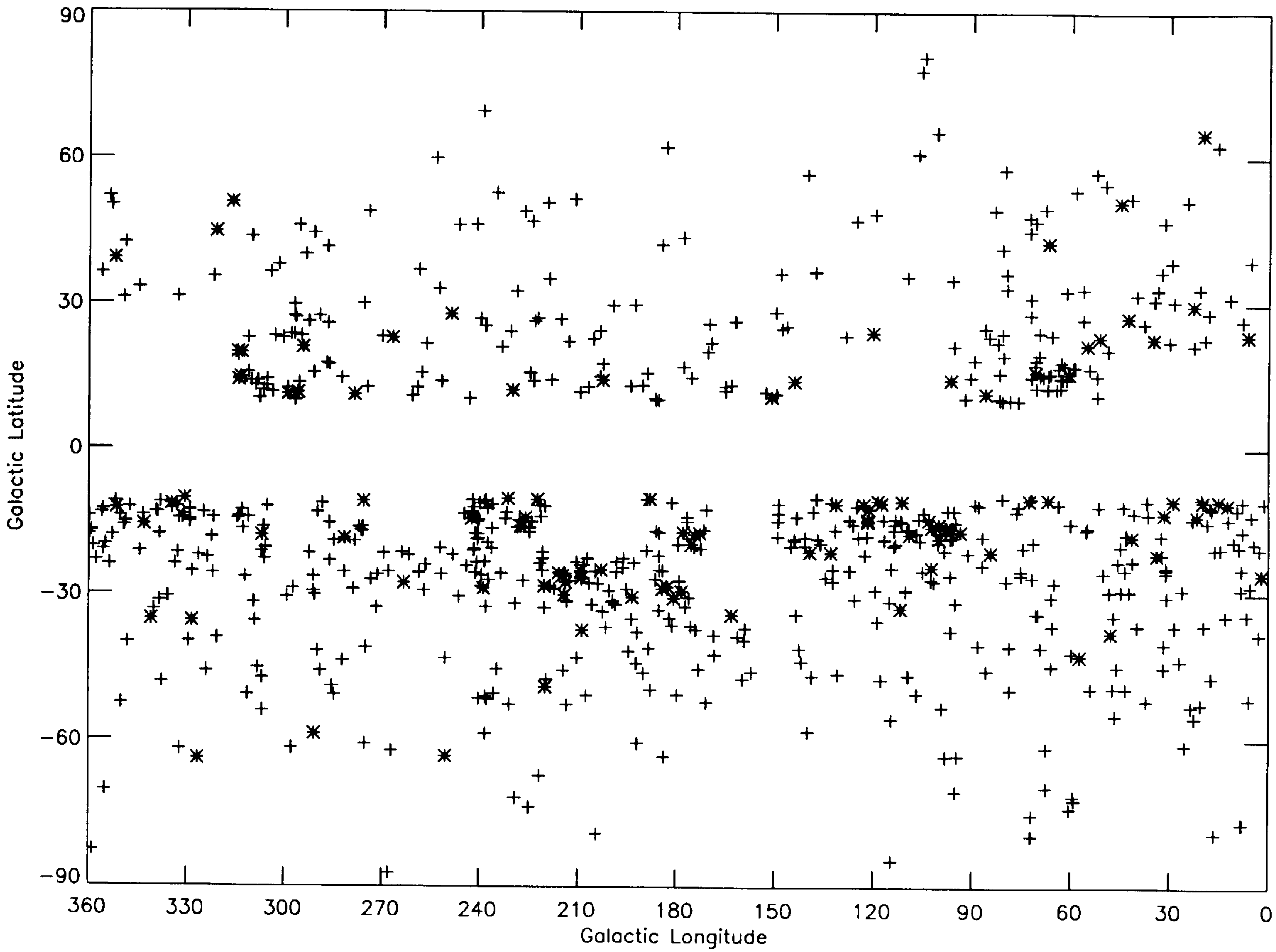
90
60
30
0
−30
−60
−90
Galactic Latitude
360
330
300
270
240
210
180
150
120
90
60
30
0
Galactic Longitude

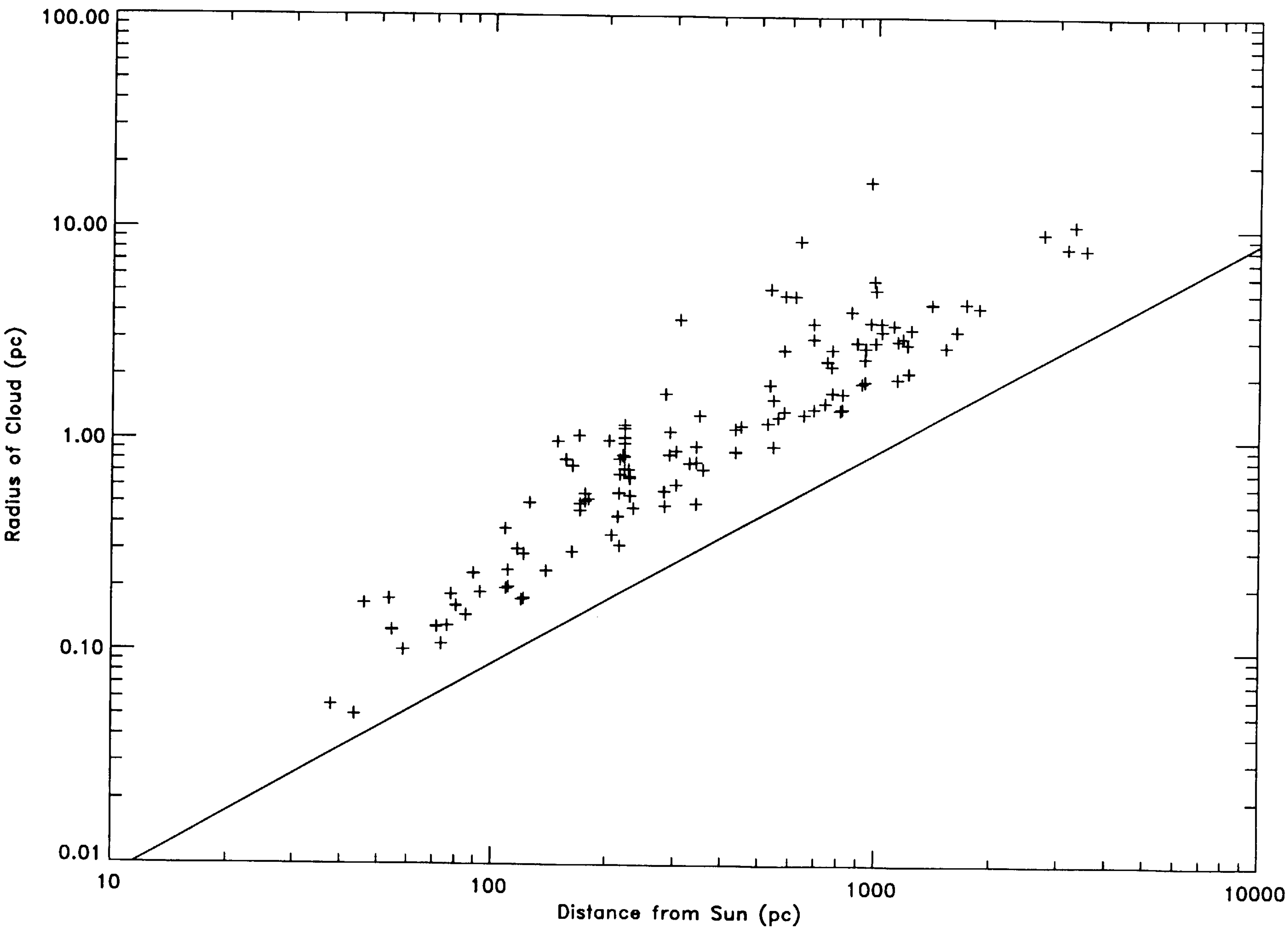

100.00
10.00
1.00
0.10
0.01
Radius of Cloud (pc)
10
100
1000
10000
Distance from Sun (pc)

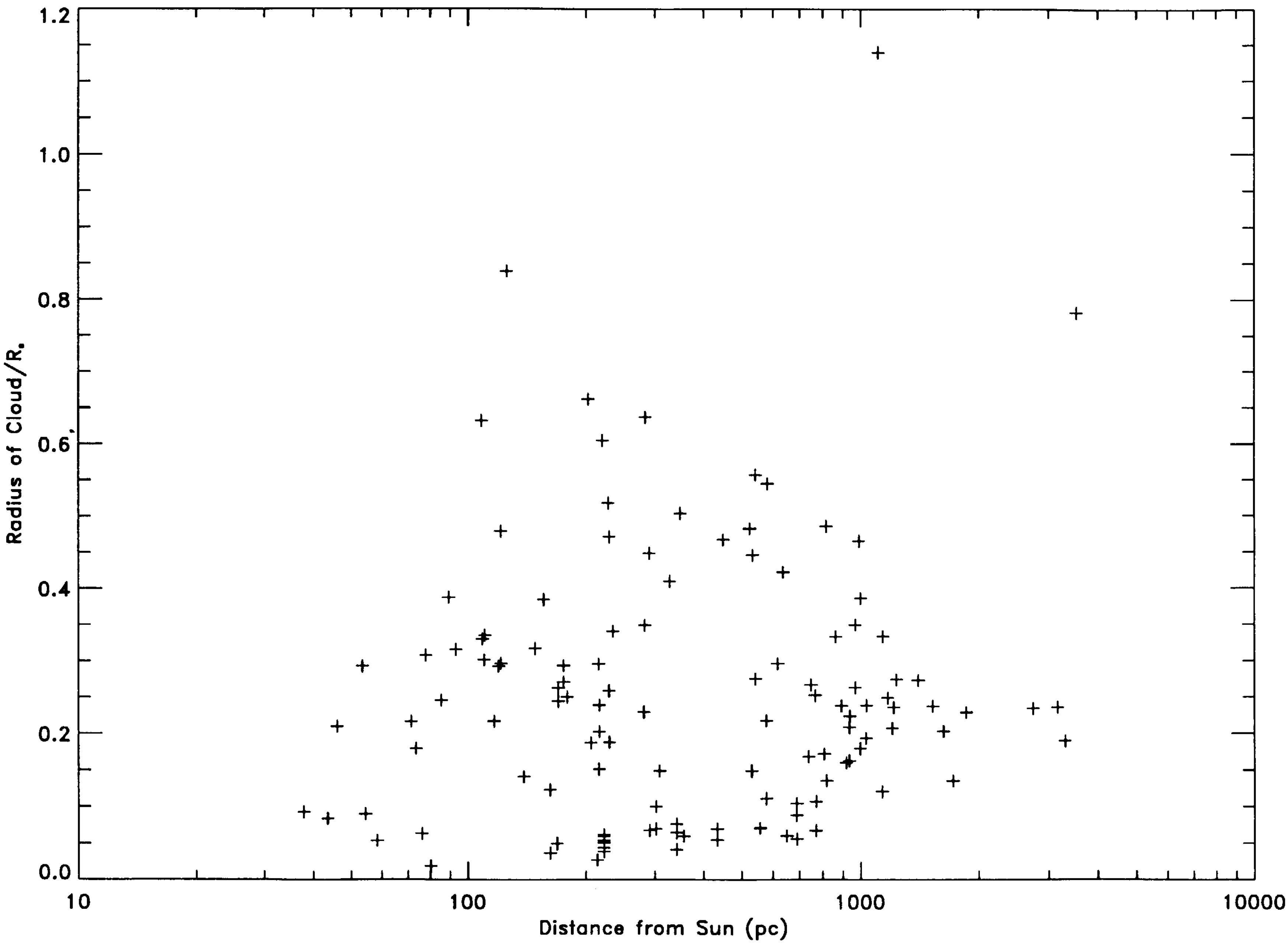
Radius of Cloud/R.
Distance from Sun (pc)
1.2
1.0
0.8
0.6
0.4
0.2
0.0
10
100
1000
10000

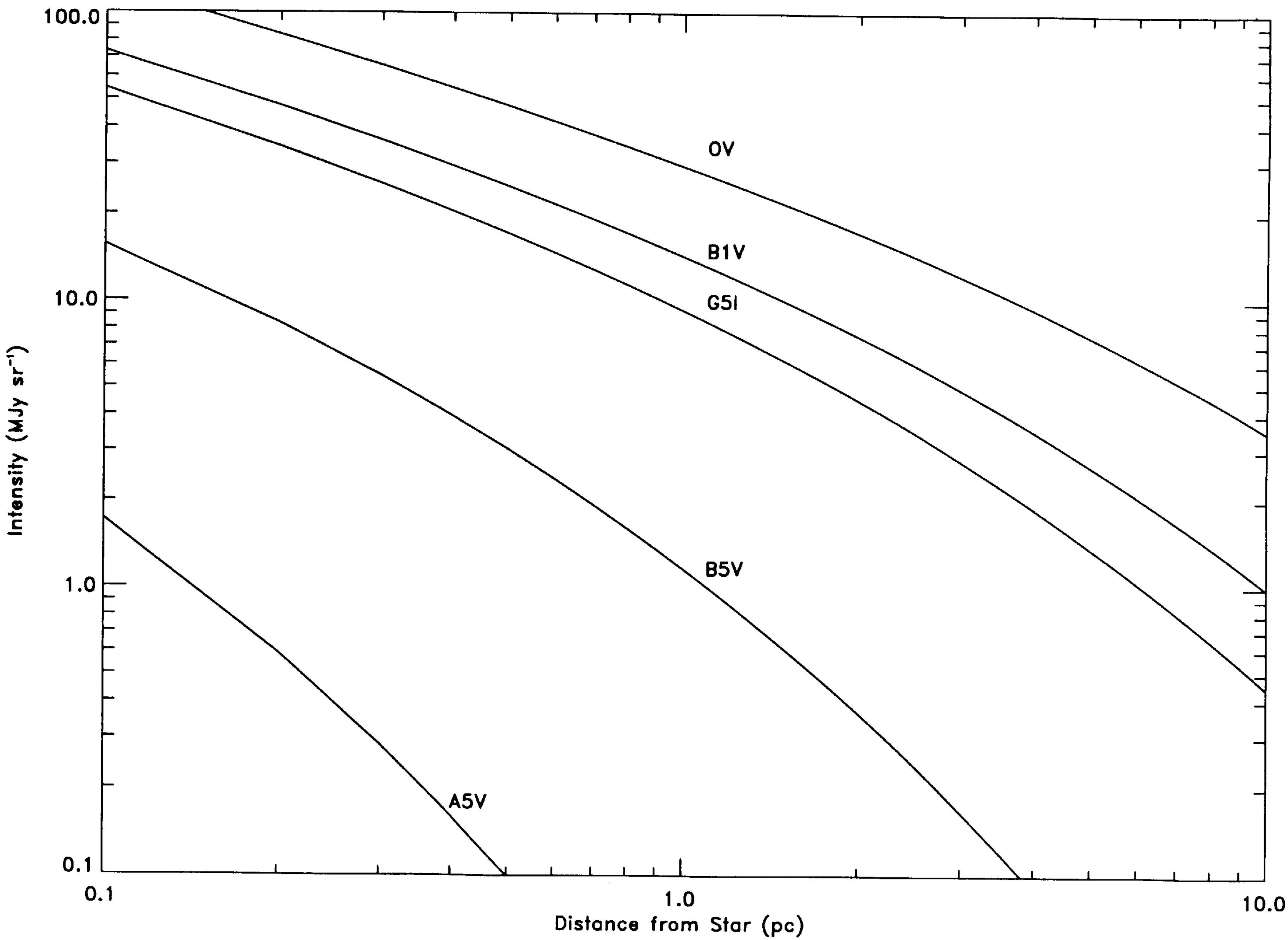

100.0
10.0
1.0
0.1
Intensity (MJy sr⁻¹)
0.1
1.0
10.0
Distance from Star (pc)
OV
B1V
G5I
B5V
A5V

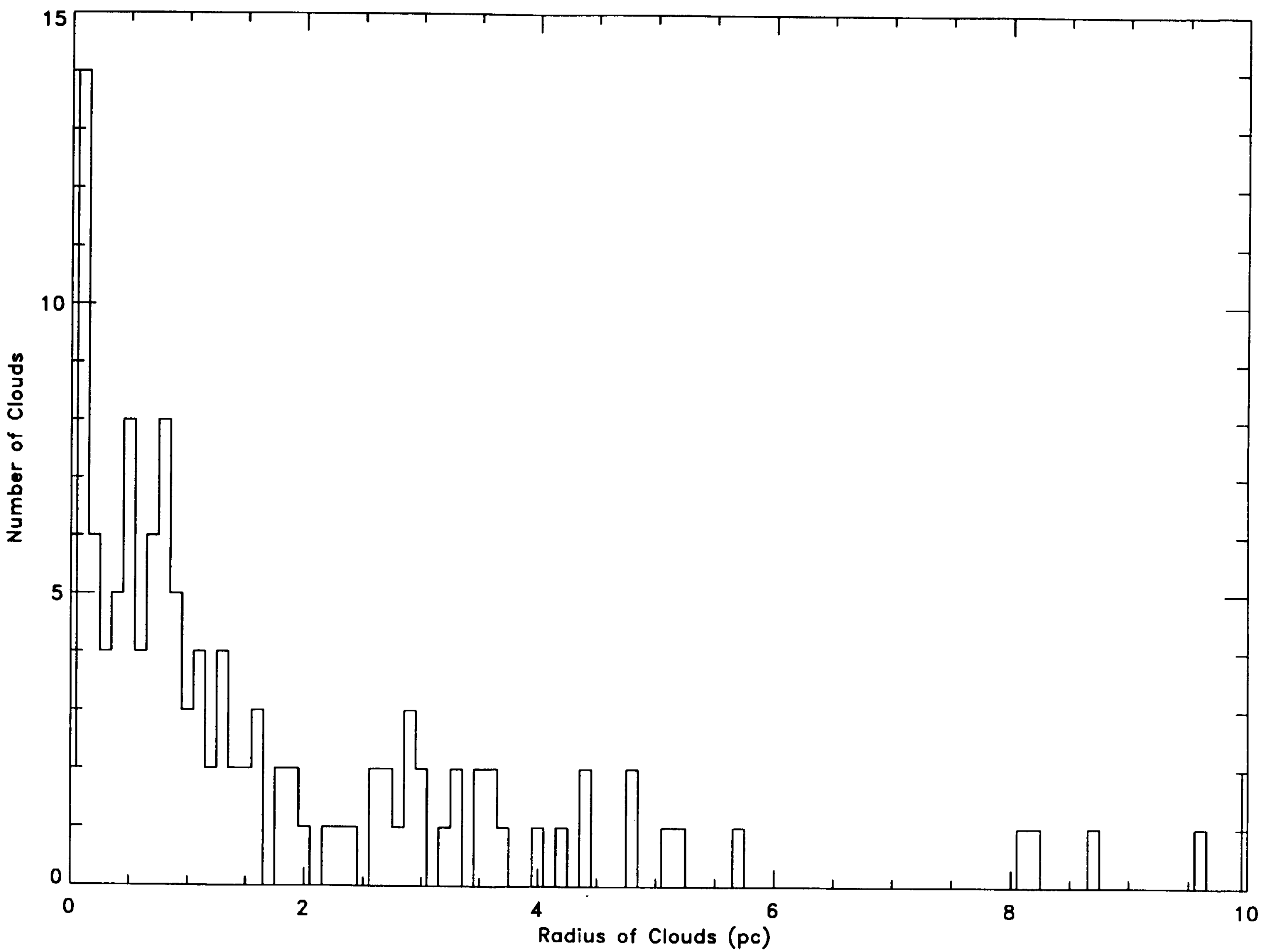
Number of Clouds
Radius of Clouds (pc)
0
5
10
15
0
2
4
6
8
10

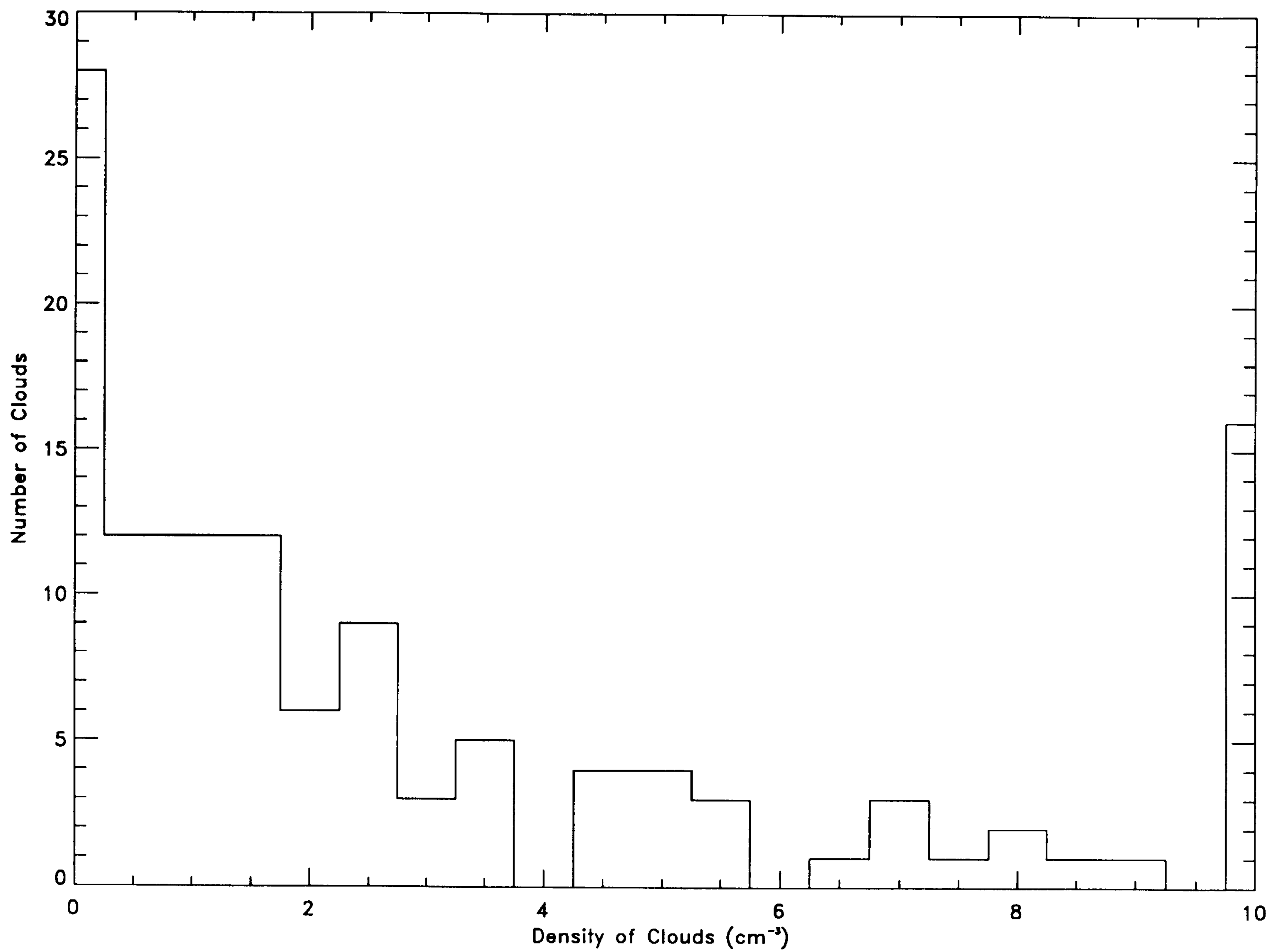
Number of Clouds
Density of Clouds (cm⁻³)
0
5
10
15
20
25
30
0
2
4
6
8
10

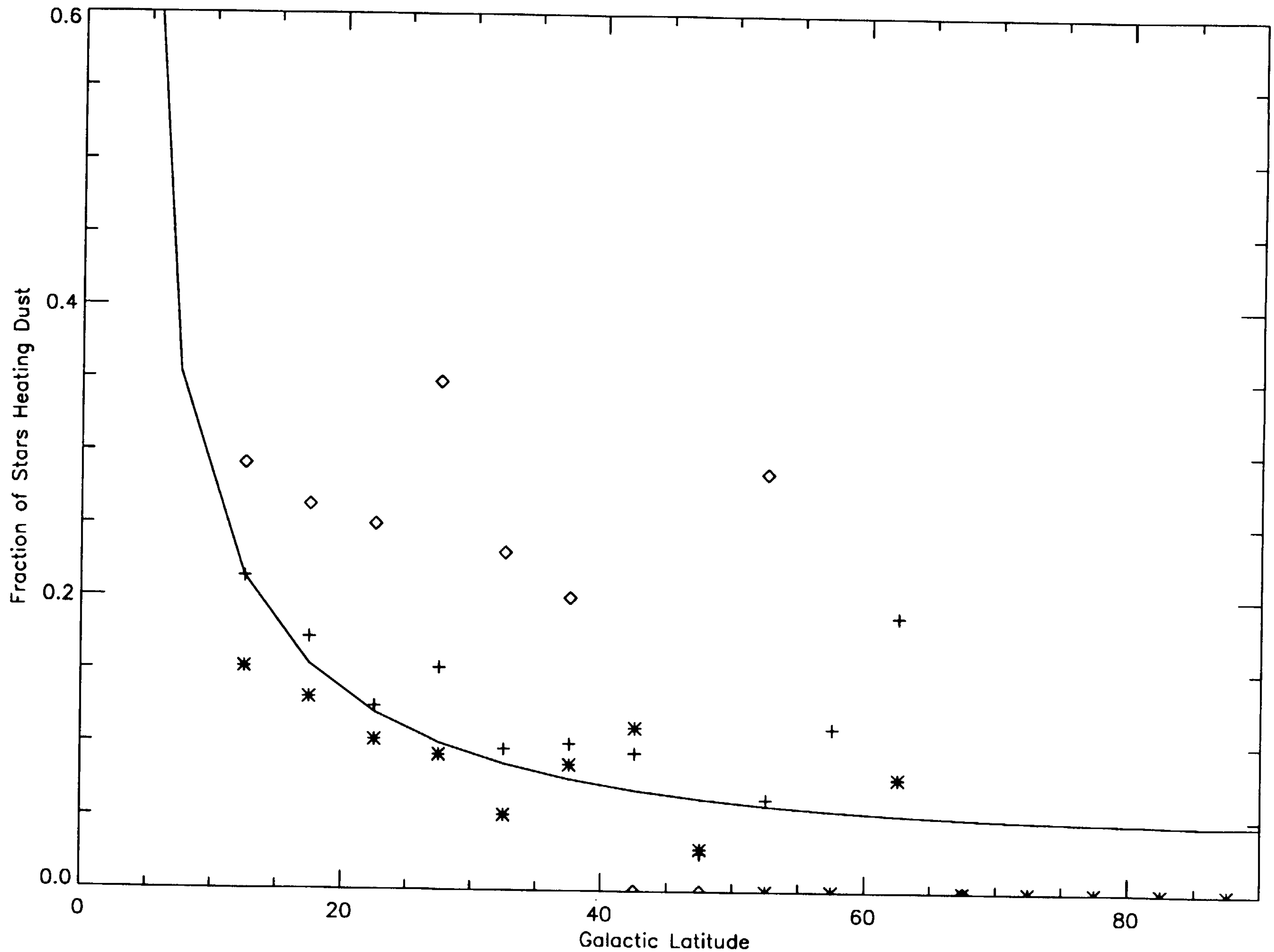

Fraction of Stars Heating Dust
0.0
0.2
0.4
0.6
0
20
40
60
80
Galactic Latitude

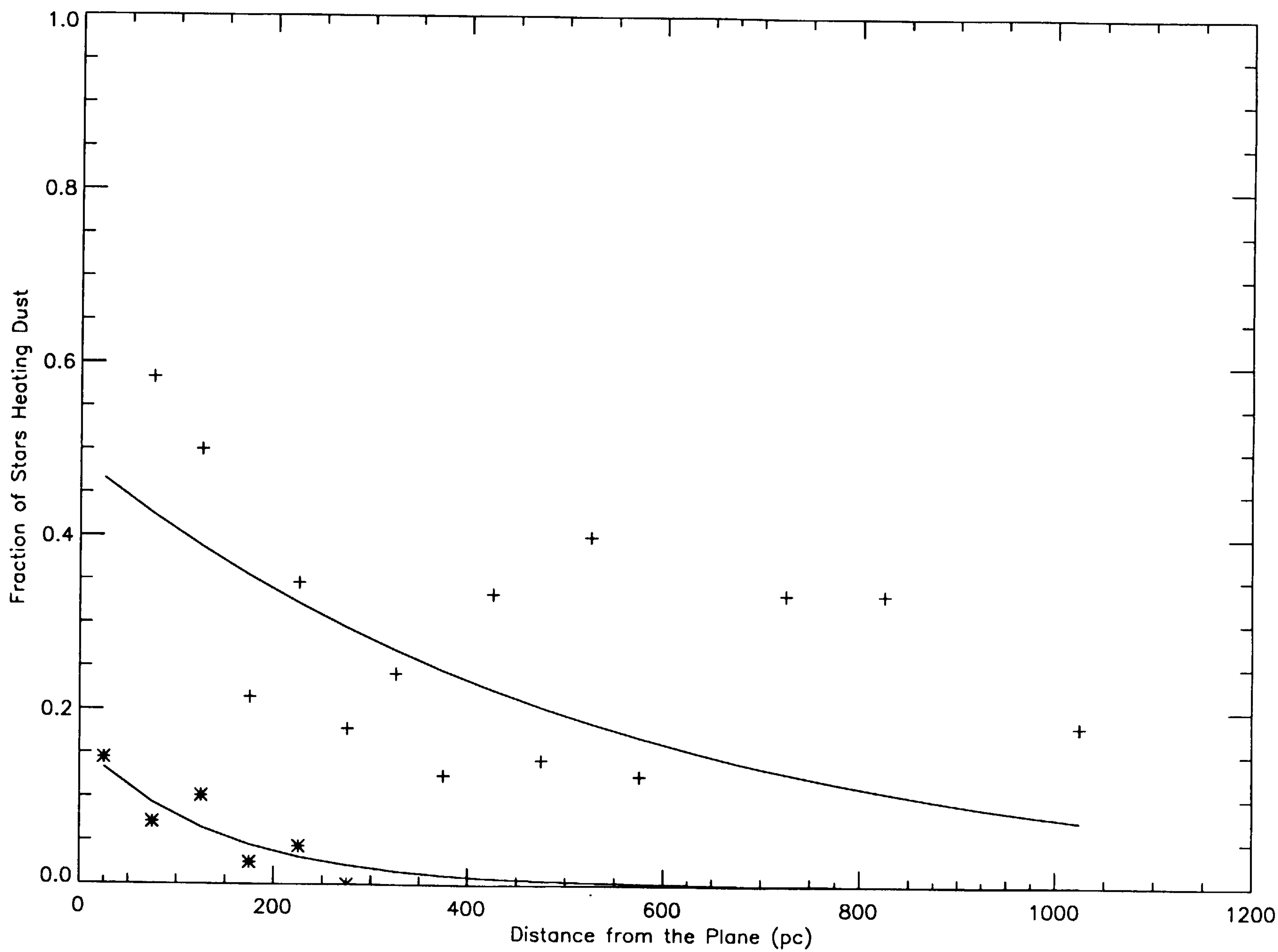

1.0
0.8
0.6
0.4
0.2
0.0
Fraction of Stars Heating Dust
0
200
400
600
800
1000
1200
Distance from the Plane (pc)

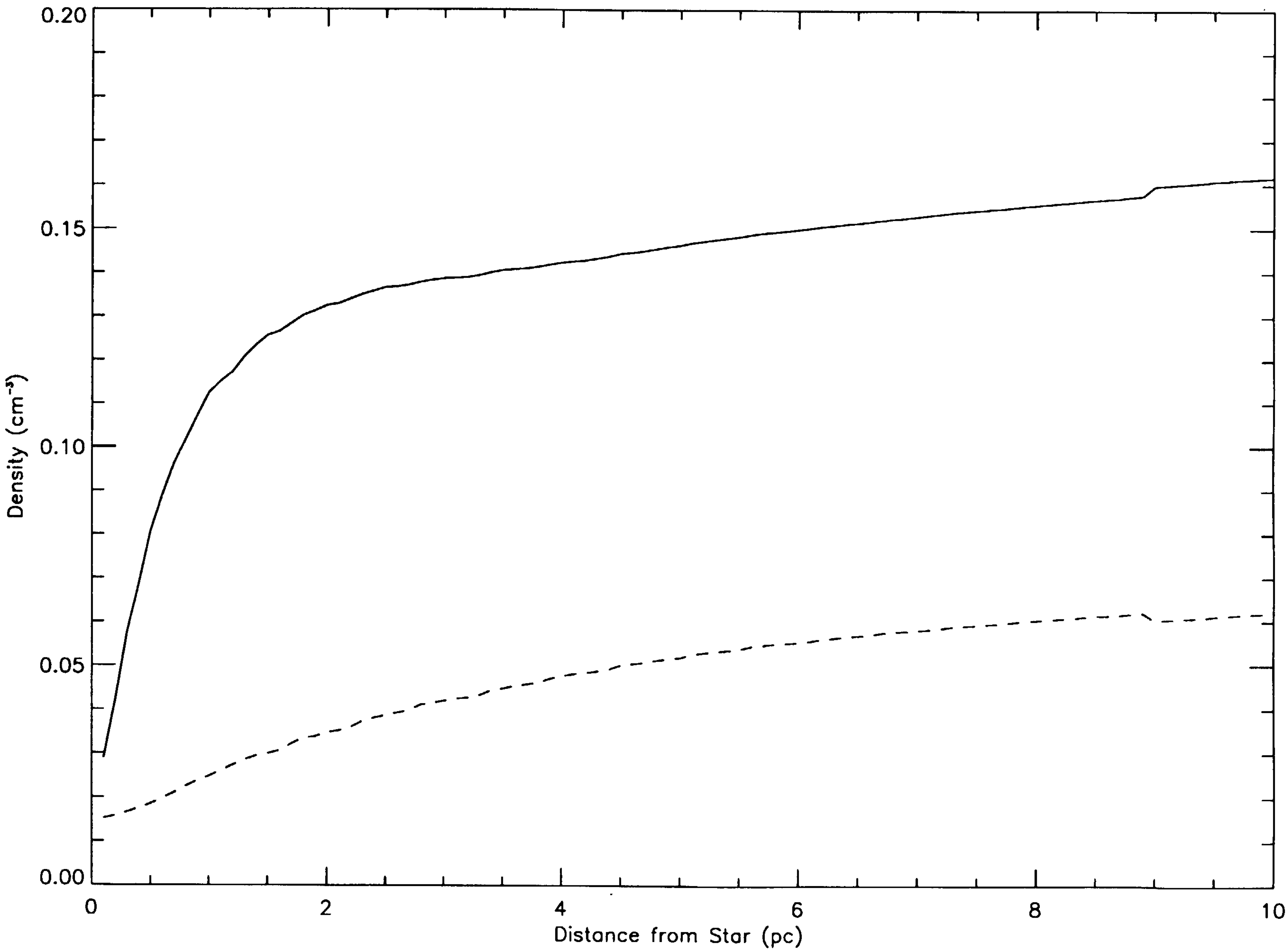
0.20
0.15
0.10
0.05
0.00
Density (cm^{-3})
0
2
4
6
8
10
Distance from Star (pc)

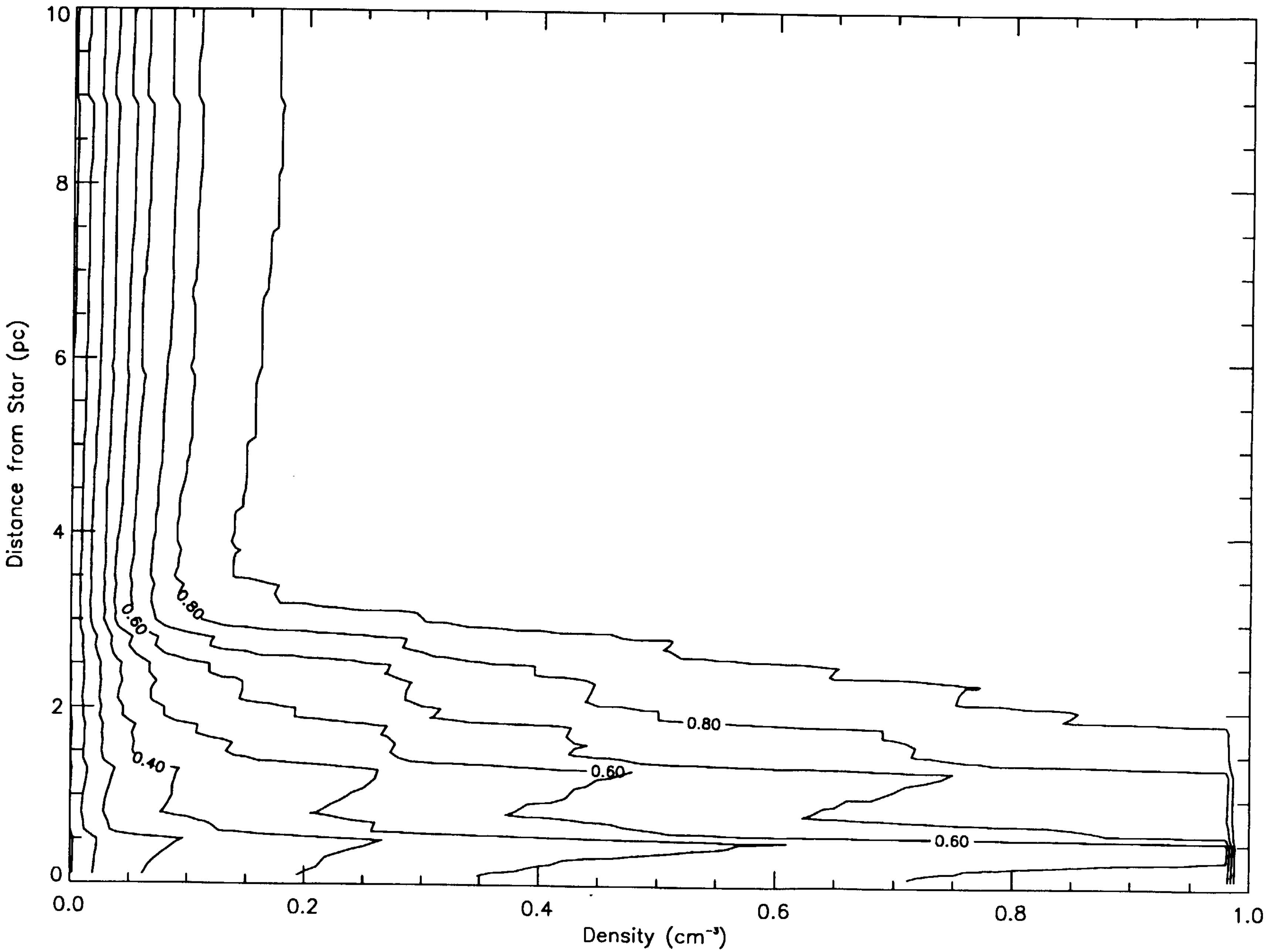

Distance from Star (pc)
Density (cm⁻³)
0.80
0.60
0.40
0.80
0.60
0.60

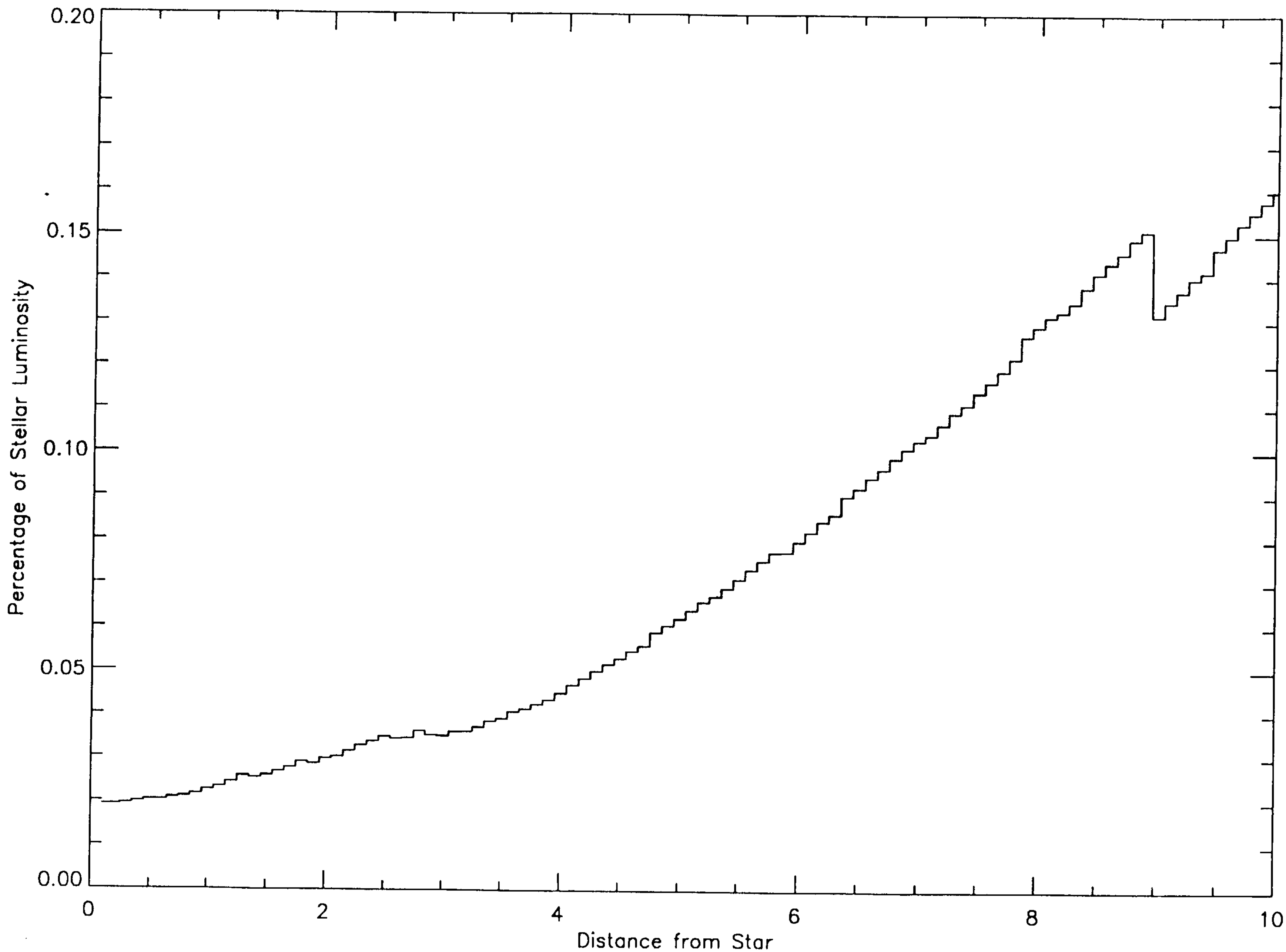
0.20
0.15
0.10
0.05
0.00
Percentage of Stellar Luminosity
0
2
4
6
8
10
Distance from Star